



Supplementary Information for

The Rise of Biting During the Cenozoic Fueled Reef Fish Body Shape Diversification

Katherine A. Corn*, Sarah T. Friedman, Edward D. Burress, Christopher M. Martinez, Olivier Larouche, Samantha A. Price, & Peter C. Wainwright

*corresponding author: Katherine A. Corn
Email: kacorn@ucdavis.edu

This PDF file includes:

Supplementary text
Figures S1 to S6
Tables S1 to S5
Legend for Dataset S1 and S2
SI References

Other supplementary materials for this manuscript include the following:

Dataset S1
Dataset S2

Supplementary Information Text

Supplemental Methods

Feeding mode categorizations. We used a hierarchical process to categorize prey proportions: where volumetric data of consumer stomach contents were available, then proportions of volume were used. If volumetric data were not available but individual counts of prey items from stomach contents were available, then proportions of the total number of prey were used. If only lists of prey taxa found in gut contents were available, then we used the proportion of taxa on which the species feeds listed to estimate proportions of prey. In this case, prey items at the end of a long list of taxa were considered less important than prey items at the beginning of the list.

History of feeding modes. We used *make.simmap* to reconstruct ancestral character states using the R package ‘phytools’ (1). We set the function to fit a continuous-time Markov model for the evolution of feeding modes using a fixed value of the Q matrix (2, 3), and we estimated the stationary distribution (π_i) from the Q matrix, which was used as the prior on the root frequency.

Random forest models. We used 7 continuous variables in each decision tree. We selected this number after iterating random forest model-fitting over different numbers of variables (ranging from 1-7), each across 5,000 decision trees, and comparing predicted group membership accuracy across the different numbers of variables used for the decision trees. We used a conditional implementation of *varimp* in the ‘party’ R package to estimate variable importance. In the conditional implementation, the importance of each trait is computed by permuting other variables whose covariance with the variable of interest exceeds a user-specified threshold (0.2 in our model) (4-7).

Hypervolumes. We used six PC axes to generate hypervolumes as hypervolumes are best run on orthogonal data axes (8) and constructed hypervolumes using the R package ‘hypervolume’ (8, 9). Each hypervolume was computed by generating a gaussian density kernel containing 95% of points from the original group of data. To assess how extreme our data were compared to a random distribution of hypervolumes, we permuted group assignments among original species data and re-computed all hypervolumes and all hypervolume comparisons. We ran 10,000 iterations of the permuted hypervolumes and comparisons between them, then compared the proportion of our comparisons between hypervolumes that were more extreme than comparisons between the distribution of analogous hypervolumes. We estimated whether our data were more extreme than the ‘null’ distribution in a 2-tailed fashion, such that our data could be more extreme than the distribution of permuted hypervolumes by occupying either more or less unique space than 95% of the distribution.

Evolutionary rate models. We set a log-normal prior on each branch’s background rate. We placed a log-uniform prior at 1×10^{-10} on the rate of transitions between states (“lambda”). To ensure that model fitting was not affected strongly by the transition rate prior, we also fit models with higher (1×10^{-7}) and lower (1×10^{-13}) priors on lambda. Both alternative prior models ran for 150,000 generations of the MCMC. Scripts are available in the supplemental information on Dryad.

Supplemental Results

History of feeding mode. Stochastic character mapping recovered asymmetrical transitions between states (Fig. S2), with many transitions between attached prey biting and mixed feeding; fewer but still numerous transitions between mixed feeding and suction feeding; some transitions between attached prey biting and suction feeding; and few transitions from suction to ram biting. We recovered almost no transitions from ram biting to any other state, and zero transitions from ram biting to either attached prey biting or mixed suction and biting.

Evolutionary rate models. A Bayesian, state-dependent, relaxed-clock model of evolutionary rate estimated 214 transitions between feeding mode states. We uncovered substantial variation in background rate across the history of body shape, as the standard deviation of the background rate parameter was relatively large (1.41). Alternative prior testing on lambda, the rate of transitions between states, revealed minimal effects of the prior (Fig. S6). There was little difference across alternative priors in any of three relevant metrics: 1) the estimated number of transitions between states, 2) the posterior estimate of lambda, or 3) the resulting ratio of rate estimates between groups of interest.

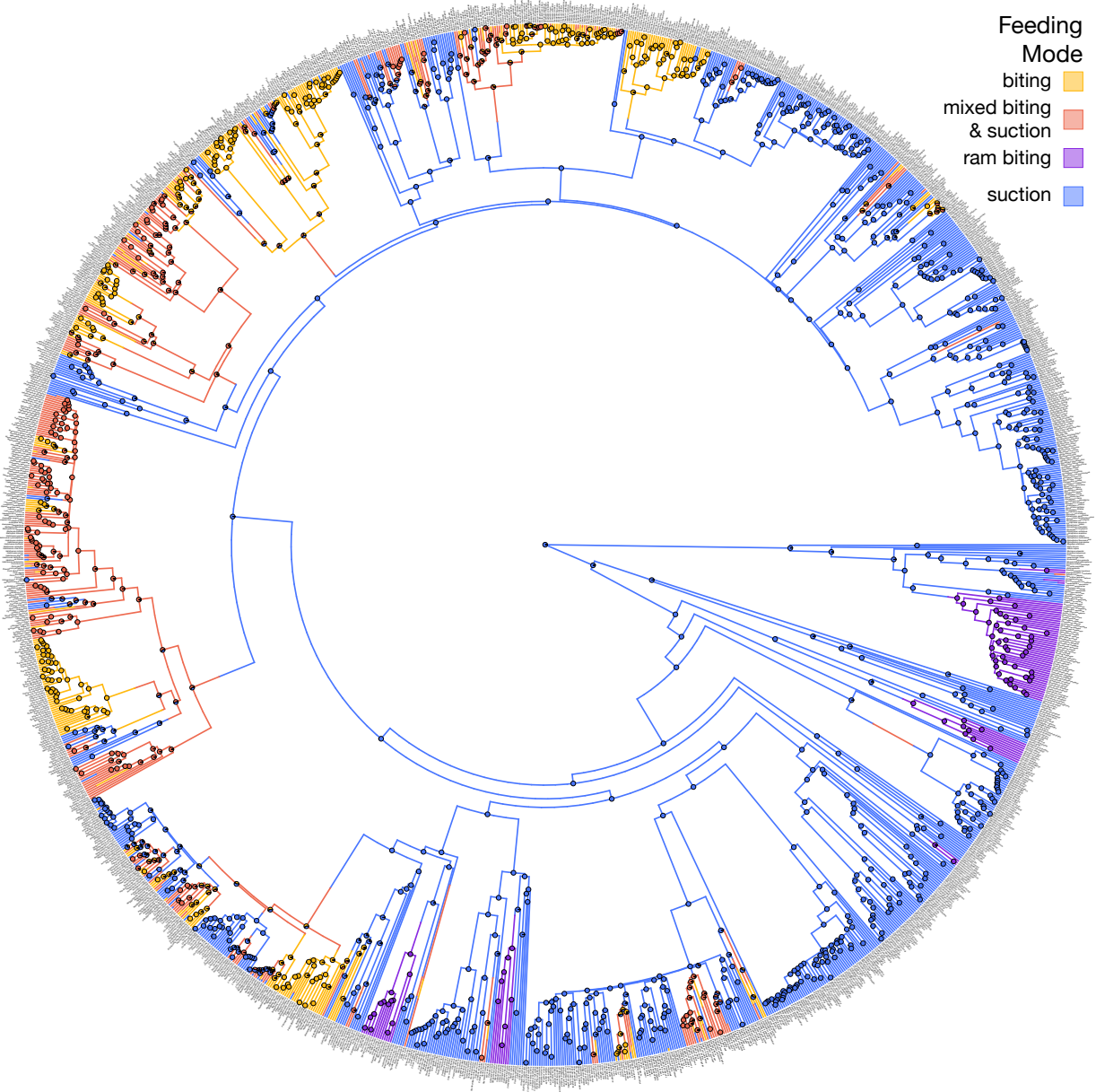


Fig. S1. A sample stochastic character map showing a simulated character history of feeding mode, with tips labeled by species. Branch mapping shown is a single map chosen at random, but pie charts at nodes summarize estimated states at each node over the full distribution of 100 stochastic character maps.

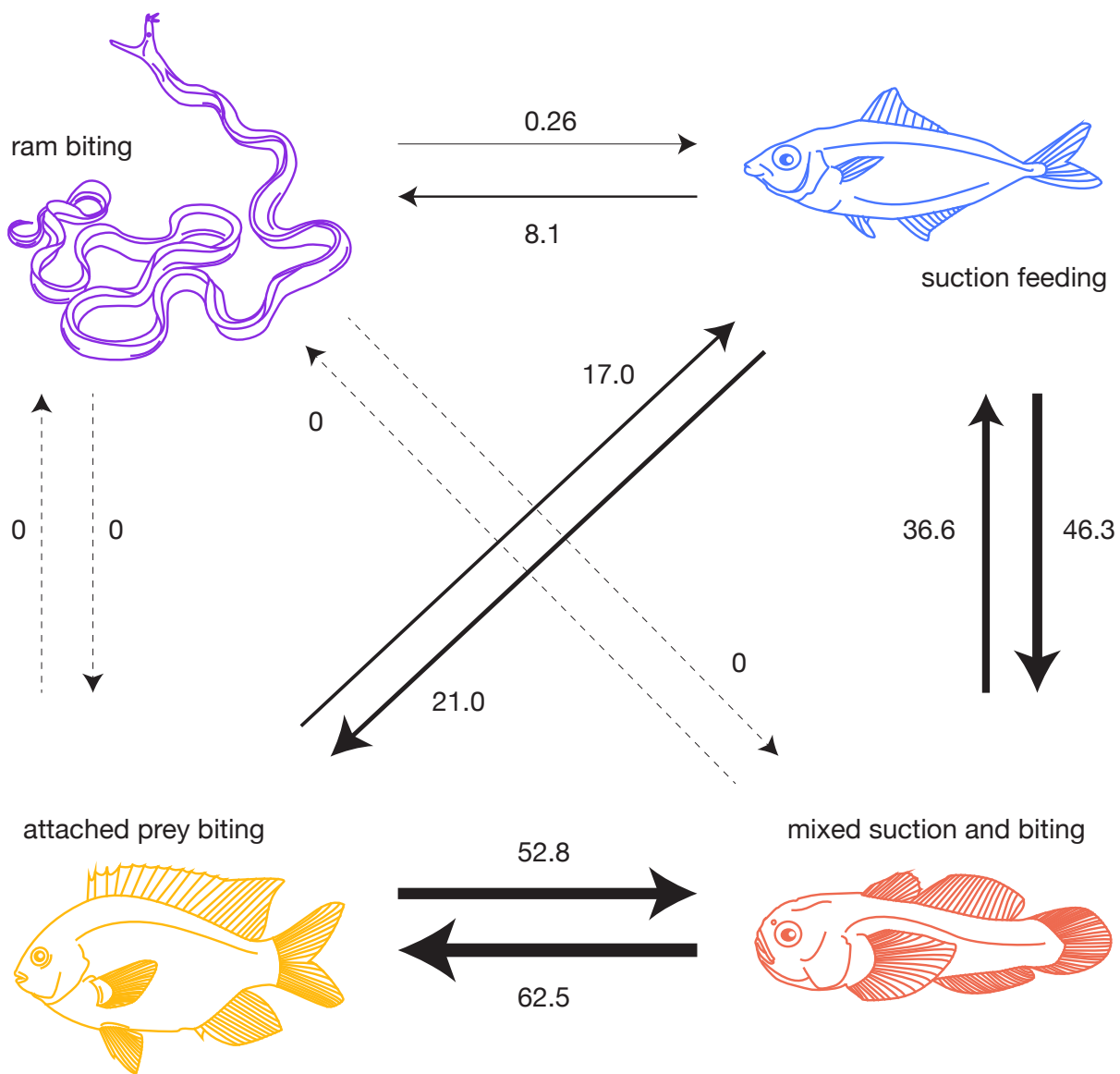


Fig. S2. Transition rate matrix between character states, from a distribution of 100 stochastic character mappings. Thickness of arrows and number beside each arrow indicates the number of transitions between the two indicated states. Notably, there are no transitions from either attached prey biting or mixed suction and biting to ram biting, and there are almost no transitions from ram biting to any other state.

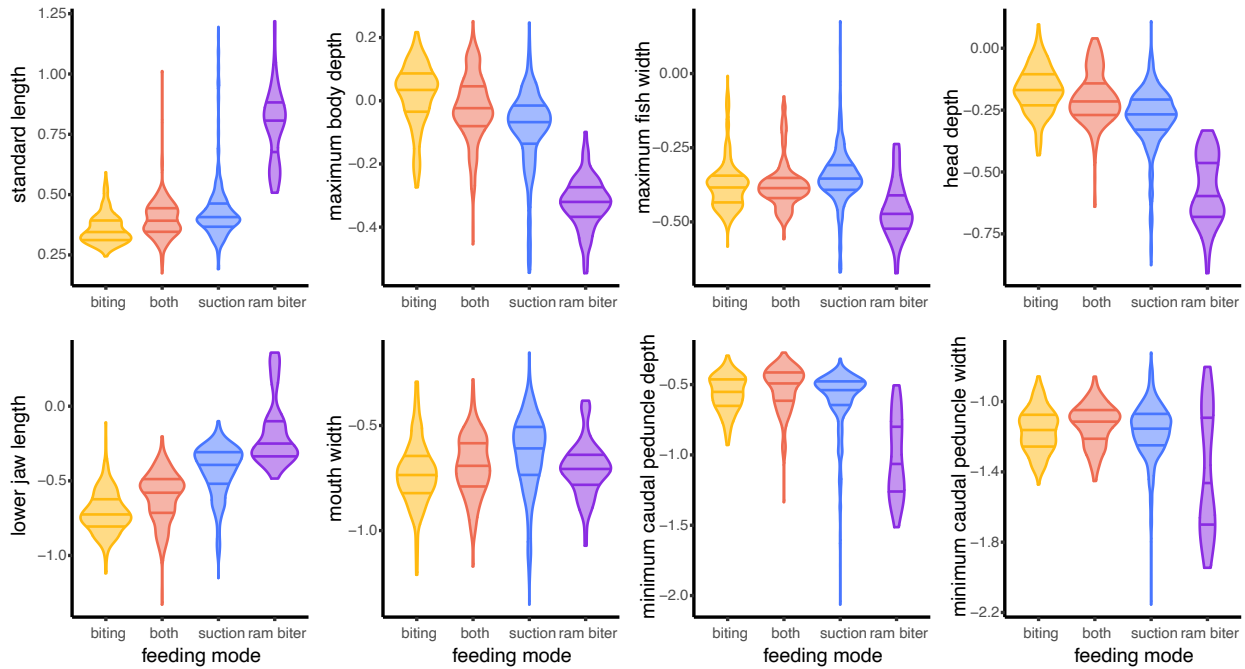


Fig. S3. Distributions of morphological traits by feeding mode. All traits were different in univariate phylogenetic ANOVAs at $\alpha = 0.05$. Only fish width was not significantly different between feeding mode groups at $\alpha = 0.01$.

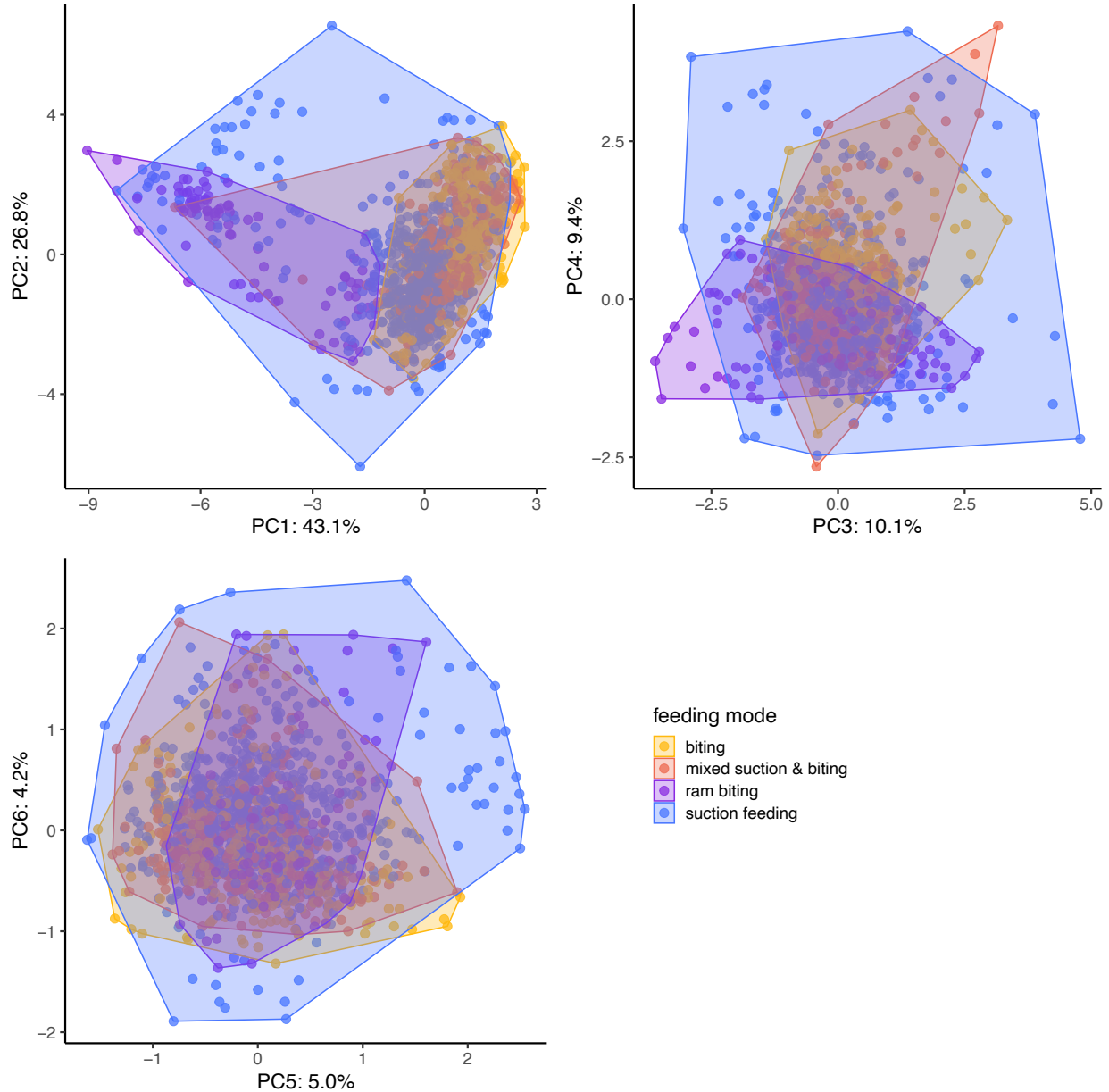


Fig. S4. Data used for generating 6-dimensional hypervolumes (principal components 1-6) plotted bivariately with convex hulls to demonstrate unique shape space occupation; together these six axes account for 98.5% of the variance in the data. Each point represents a species; points and convex hulls are colored by feeding mechanism. The primary region of unique shape space occupation by biters and mixed feeders lies along the right margin of PC1, and includes a range of species from several families using biting or mixed suction and biting, such as *Monacanthus chinensis*, *Acanthurus coeruleus*, *Canthigaster janthinoptera*, *Platax batavianus*, and *Pervagor janthinosoma*. These fishes are characterized by laterally compressed, shortened bodies with small mouths.

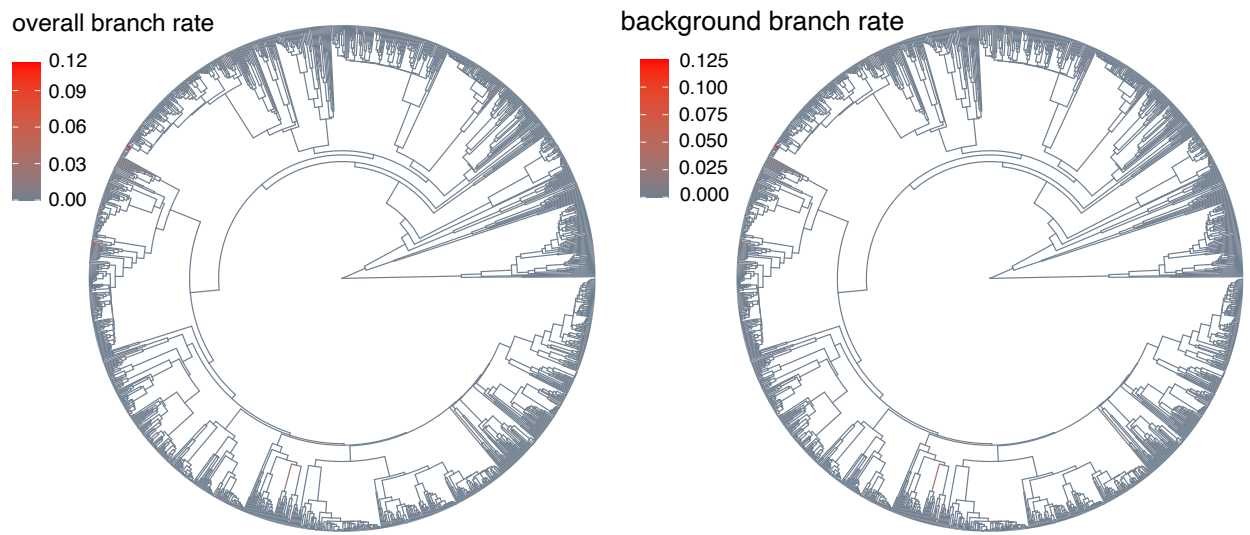


Fig. S5. Additional branch-specific rates of evolution from evolutionary model-fitting. Left, overall branch rates plotted onto the phylogeny, calculated as the product of state-dependent rates and background rates for each branch. Right, background rates, which absorb rate variation not attributed to feeding mode. Homogeneity of background rates on a broader scale suggests that a small number of short branches have elevated rates in comparison to longer branches clades, a pervasive phenomenon in evolutionary rate modeling (10).

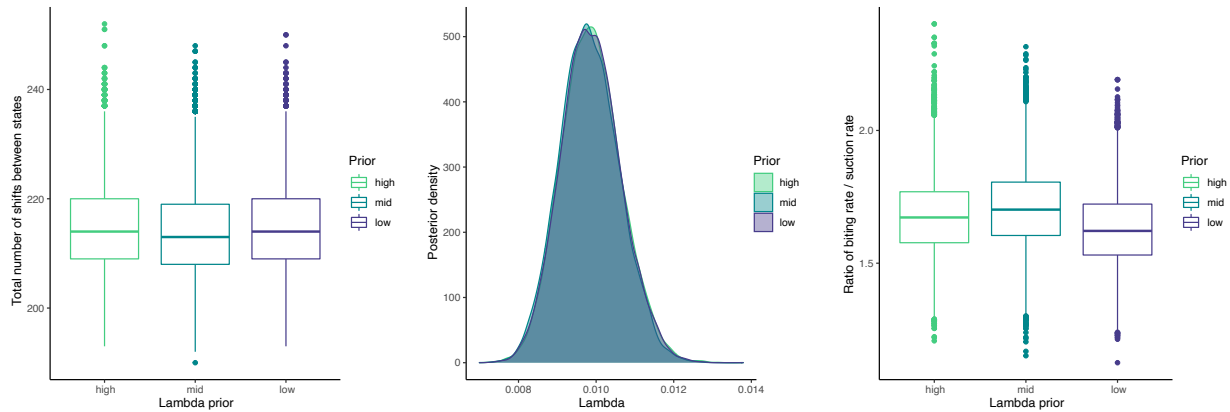


Fig. S6. Relevant statistics from alternative prior testing on the log uniform prior on the number of state changes for evolutionary rate modeling. Left, total number of transitions between discrete character states; center, estimate of lambda, the transition rate parameter; and right, sample of rates of continuous character evolution in different discrete states shown as a rate ratio of “biting” group and “suction” group. The model using the “mid” prior was used for interpretation of results in the main text.

Table S1. Loadings from a principal component analysis on the correlation matrix.

Trait	PC1	PC2	PC3	PC4	PC5	PC6	PC7	PC8
Standard length	-0.50	0.09	-0.32	0.06	-0.08	-0.27	0.32	-0.07
Maximum body depth	0.46	0.27	0.08	-0.33	0.15	0.027	-0.45	-0.06
Maximum fish width	0.12	-0.54	0.41	0.40	-0.10	0.40	0.14	-0.04
Head depth	0.49	0.11	0.03	-0.13	0.32	-0.10	0.78	5.55×10^{-17}
Lower jaw length	-0.23	-0.40	-0.26	-0.66	0.22	0.48	0.07	-2.78×10^{-17}
Mouth width	0.01	-0.59	0.21	-0.19	0.21	-0.71	-0.14	2.08×10^{-16}
Minimum caudal peduncle depth	0.39	-0.22	-0.33	-0.20	-0.79	-0.11	0.08	-5.55×10^{-17}
Minimum caudal peduncle width	0.28	-0.25	-0.70	0.45	0.36	0.03	-0.19	8.33×10^{-17}
Cumulative variance explained	0.43	0.70	0.80	0.90	0.94	0.98	1.00	1.00

Table S2. Results from phylogenetic ANOVAs.

Regression	d.f.	p-value	r ²	Z score
Standard length ~ feeding mode	3, 1526	p < 0.01	0.0084	1.88
Maximum body depth ~ feeding mode	3, 1526	p < 0.0001	0.021	2.84
Maximum fish width ~ feeding mode	3, 1526	p < 0.05	0.0074	1.77
Head depth ~ feeding mode	3, 1526	p < 0.001	0.010	2.12
Lower jaw length ~ feeding mode	3, 1526	p < 0.0001	0.062	3.82
Mouth width ~ feeding mode	3, 1526	p < 0.01	0.010	2.02
Minimum caudal peduncle depth ~ feeding mode	3, 1526	p < 0.0001	0.022	2.89
Minimum caudal peduncle width ~ feeding mode	3, 1526	p < 0.0001	0.021	2.80
All traits ~ feeding mode (MANOVA)	3, 1526	p < 0.0001	0.028	5.98

Table S3. Random forest results.

Trait	Importance (weighted mean decrease in accuracy when trait is excluded)
Lower jaw length	0.201
Head depth	0.0533
Standard length	0.0401
Minimum caudal peduncle depth	0.0307
Maximum body depth	0.00500
Minimum caudal peduncle width	0.00448
Maximum fish width	0.00275
Mouth width	0.00149

Table S4. Morphological disparity results, computed using *geomorph*.

Trait	Biters variance	Mixed suction & biting variance	Ram biting variance	Suction variance
Standard length	0.0037	0.0060	0.022	0.020
Maximum body depth	0.0098	0.011	0.0063	0.015
Maximum fish width	0.0071	0.0064	0.0086	0.0081
Head depth	0.0088	0.011	0.018	0.015
Lower jaw length	0.019	0.028	0.049	0.028
Mouth width	0.023	0.021	0.016818	0.033
Minimum caudal peduncle depth	0.016	0.024	0.080	0.044
Minimum caudal peduncle width	0.015	0.0135	0.12	0.025

Table S5. Hypervolume results, computed using *hypervolume*.

Hypervolume 1	Hypervolume 2	Unique fraction of hypervolume 1 (unique frac. 1)	Proportion of permuted distribution less than unique frac. 1	Unique fraction of hypervolume 2 (unique frac. 2)	Proportion of permuted distribution less than unique frac. 2
Biting	All not Biting	0.13	0.597	0.84	0.542
Mixed suction & biting	All not Mixed suction & biting	0.10	0.831	0.80	0.188
Suction	All not Suction	0.44	0.201	0.54	0.779
Ram biting	All not Ram biting	0.91	0.267	0.82	0.960
Biting + Mixed suction & biting	Suction + Ram biting	0.19	0.110	0.83	0.870

Dataset S1 (separate file, csv, available on dryad at doi: 10.25338/B8NM0K). Feeding mode categorizations for 1,530 species of reef fishes, including references.

Dataset S2 (separate file, csv, available on dryad at doi: 10.25338/B8NM0K). Body shape data for 8 linear measurements for 1,530 species of teleost fishes.

SI References

1. L. J. Revell, phytools: An R package for phylogenetic comparative biology (and other things). *Methods Ecol. Evol.* 3, 217–223 (2012).
2. J. P. Huelsenbeck, R. Nielsen, J. P. Bollback, Stochastic mapping of morphological characters. *Syst. Biol.* 52, 131–158 (2003).
3. J. P. Bollback, SIMMAP: Stochastic character mapping of discrete traits on phylogenies. *BMC Bioinformatics* 7 (2006).
4. C. Strobl, A. L. Boulesteix, A. Zeileis, T. Hothorn, Bias in random forest variable importance measures: Illustrations, sources and a solution. *BMC Bioinformatics* 8 (2007).
5. T. Hothorn, K. Hornik, A. Zeileis, Unbiased recursive partitioning: A conditional inference framework. *J. Comput. Graph. Stat.* 15, 651–674 (2006).
6. T. Hothorn, B. Lausen, A. Benner, M. Radespiel-Tröger, Bagging survival trees. *Stat. Med.* 23, 77–91 (2004).
7. C. Strobl, A. L. Boulesteix, T. Kneib, T. Augustin, A. Zeileis, Conditional variable importance for random forests. *BMC Bioinformatics* 9, 1–11 (2008).
8. B. Blonder, *et al.*, New approaches for delineating n-dimensional hypervolumes. *Methods Ecol. Evol.* 9, 305–319 (2018).
9. B. Blonder, C. Lamanna, C. Violle, B. J. Enquist, The n-dimensional hypervolume. *Glob. Ecol. Biogeogr.* 23, 595–609 (2014).
10. L. J. Harmon, *et al.*, Causes and Consequences of Apparent Timescaling Across All Estimated Evolutionary Rates. *Annu. Rev. Ecol. Evol. Syst.*, 587–609 (2021).